Proceedings of the JMSM 2008 Conference

First principles calculations of structural, electronic and thermodynamic properties of SrS, SrSe, SrTe compounds and SrS$_{1-x}$Se$_x$ alloy

S. Labidi[a]*, H. Meradji[a], M. Labidi[a], S. Ghemid[a], S. Drablia[a] and F. El Haj Hassan[b]

[a] *Laboratoire de Physique des Rayonnements, Département de Physique, Faculté des Sciences, Université de Annaba, Algeria*
[b] *Laboratoire de Physique des Matériaux, Faculté des Sciences, Université Libanaise, Elhadath, Beirut, Lebanon*

Abstract

The ab initio full potential linearized augmented plane wave (FP-LAPW) method within density functional theory was applied to study the structural and electronic properties of the compounds SrS, SrSe, SrTe and their alloy SrS$_{1-x}$Se$_x$ in the NaCl structure. Results are obtained using both the local density approximation (LDA) and the generalized gradient approximation (GGA) for the exchange-correlation potentials. The ground-state properties, like lattice constant and bulk modulus obtained from our calculations agree very well with experimental and other theoretical calculations. We present the main features of electronic properties, where the electronic band structure shows that the fundamental energy gap is indirect ($\Gamma \rightarrow X$). Moreover the alternative form of GGA proposed by Engel and Vosko (GGA-EV) is also used for band structure calculations. Results obtained with this approximation show that significant improvement over other theoretical work are closer to the experimental data. The effect of composition on lattice parameter and bulk modulus was investigated.
Deviations of the lattice constant from Vegard's law and the bulk modulus from linear concentration dependence were observed for the alloy. Moreover, the microscopic origins of the gap bowing were explained. In addition the thermodynamic stability of the alloy was investigated by calculating the critical temperature for SrS$_{1-x}$Se$_x$ alloy.

1. Introduction

The II–VI compound semiconductors have recently received considerable interest from both experimental and theoretical points of view [1]. This is due to their potential technological applications from the blue to the near-ultraviolet spectral region. Among these compounds, the strontium chalcogenides SrX (X=S, Se and Te), together

_____

* S. Labid. Tel.: 0662058490; fax: 038875399.
E-mail address: labidisalima@yahoo.fr.

with other alkaline earth chalcogenides form a very important closed shell ionic system with NaCl crystal structure at normal conditions. They are technologically important materials, with applications in the area of luminescent devices, radiation dosimetry, fast high-resolution optically stimulated luminescence imaging, and infrared sensitive devices [2–4]. Under higher pressure prior to metallization, they undergo a first order structural phase transition to CsCl structure [5]. Semiconductor alloys, which are solid solutions of two or more semiconducting elements, have important technological applications, especially in the manufacture of electronic and electro-optical devices [6]. One of the easiest ways to change artificially the electronic and optical properties of semiconductors is by forming their alloy. It is possible to combine two different compounds with different optical band gaps and different rigidities in order to obtain a new material with intermediate properties. Concerning the alloy, to the best of our knowledge no experimental or theoretical investigations of $SrS_{1-x}Se_x$ ternary alloy has appeared in the literature Therefore, the purpose of this paper is to study the structural and electronic properties of SrS and SrSe compounds as well as to investigate the disorder effects in the strontium alloy $SrS_{1-x}Se_x$ using the full potential linearized augmented plane wave (FP-LAPW) method. The physical origins of gap bowing are investigated by following the approach of Zunger and co-workers [7]. This model is capable of realistically taking into account the dominant effects of both chemical and bond length variations, unlike traditional methods like the VCA.

The paper is organized as follows: in Section 2, we describe the calculation procedure; Results are presented in Section 3; and Section 4 contains the conclusion.

2. Computational details

The calculations were performed using the full-potential linear augmented plane wave (FP-LAPW) method within the frame work of density functional theory (DFT) [8,9] as implemented in wien2k code [10]. The exchange-correlation potential for structural properties was calculated by the generalized gradient approximation (GGA) based on Perdrew et al [11], and the local density approximation based on Wang et al [12] while for electronic properties, in addition to GGA correction, Engel and Vosko GGA (EVGGA) [13] scheme was also applied. In the FP-LAPW method, the wave function, charge density and potential are expanded differently in the two regions of unit cell. Inside the non-overlapping spheres of radius R_{MT} around each atom, spherical harmonics expansion are used, while in the remaining space of the unit cell (interstitial region) a plane wave basis set is chosen. We use a parameter $R_{MT}K_{max}=8$ which determine matrix size, where R_{MT} denotes the smallest atomic sphere radius and K_{max} gives the magnitude of largest K vector in the plane wave expansion. The charge density was Fourier expanded up to $G_{max}=14$ $(Ryd)^{1/2}$. The maximum l value for the wave function expansion inside spheres was confined to $l_{max}=10$. The muffin-tin radius were chosen to be 2.2, 2.1, 2.2 and 2.4 a.u for Sr, S, Se and Te, respectively. A mesh of 47 special k-points for binary compounds and 125 special k-points for alloy were taken in the irreducible wedge of the Brillouin zone for the total energy calculation. Both the plane wave cut-off and the number of k-points were varied to ensure total energy convergence.

3. Results and discussion

3.1. Structural properties

Firstly, the structural properties of the binary compounds SrS, SrSe and SrTe in the rocksalt structure were analyzed. We model the alloy at some selected compositions with ordered structures described in terms of periodically repeated supercells with eight atoms per unit cell, for the compositions x = 0.25, x = 0.5, x = 0.75. For the structures considered, the total energies were calculated as a function of volume and were fitted to Murnaghan's equation of state [14]. The corresponding equilibrium lattice constants and bulk modulus for both binary compounds and their alloy are given in Table 1. Considering the general trend that the GGA usually overestimates the lattice parameters while LDA is expected to underestimates them [15], our GGA results for the binary compounds are in reasonable agreement with the experimental and other theoretical values. The bulk modulus for the three compounds as illustrated by the present GGA calculation is in better agreement with the theoretical data values reported in reference [21] than the previous experimental data quoted in references [19,5,20]. By the use the LDA calculation our results are in good agreement with experimental and other theoretical calculations. Hence, it could be expected

that the LDA would improve the results of the bulk modulus values for different x Se contents in SrS1-xSex. So far, to the best of our knowledge, no experimental or theoretical data has been reported.

Usually, in solving the alloy problems, it is assumed that the atoms are located at ideal lattice sites and the lattice constants of alloys should vary linearly with composition x according to Vegard's law [16], however, violations of Vegard's rule have been reported in semiconductor alloys both experimentally [17] and theoretically [18].

Table 1: Calculated lattice parameter (a) and bulk modules (B) for strontium chalcogenides and their alloy at equilibrium volume.

	Lattice constant a (Å)					Bulk modulus B (GPa)				
	Present work		expt	other calculations		Present work		expt.	other calculations	
	GGA	LDA		GGA	LDA	GGA	LDA		GGA	LDA
SrS	6.065	5.906	6.024 [a]	6.076[d]	5.926[e]	46.263	57.981	58[a]	47[d]	54[f]
SrSe	6.303	6.124	6.236 [b]	6.323[d]	6.151[e]	41.069	49.845	45 [b]	41[d]	47[f]
SrTe	6.735	6.527	6.66[c]	6.76[d]	6.543[e]	31.802	39.008	39.5[c]	36[d]	38[f]
SrS$_{0.75}$Se$_{0.25}$	6.133	5.962				45.606	55.746			
SrS$_{0.5}$Se$_{0.5}$	6.195	6.017				44.840	53.649			
SrS$_{0.25}$Se$_{0.75}$	6.251	6.071				43.496	51.519			

[a]ref [19], [b]ref [5], [c] Ref[20], [d] ref [21], [e]ref [22], [f] ref [23]

.

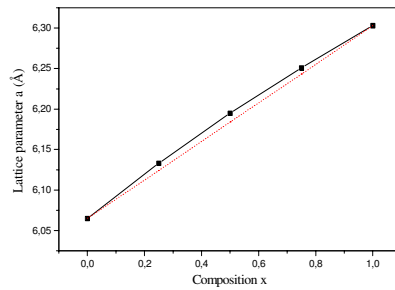Fig. 1: Composition dependence of the calculated lattice constants of SrS1-xSex alloy (solid squares) compared with Vegard's prediction (dashed line).
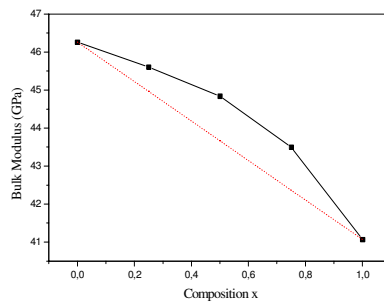

Fig. 2: Composition dependence of the calculated bulk modulus of SrS$_{1-x}$Se$_x$ alloy (solid squares) compared with LCD prediction (dashed line).

Figure1 shows the variation of the calculated equilibrium lattice constant versus concentration for $SrS_{1-x}Se_x$ alloy. A slight deviation from Vegard's law is clearly visible for the $SrS_{1-x}Se_x$ alloy with upward bowing parameter equal to -0.043 Å, obtained by fitting the calculated values with a polynomial function. The physical origin of this small deviation could be mainly due to the weak mismatch of the lattice constants of SrS and the other binary compound SrSe.

In figure2, the composition dependence of bulk modulus is compared to the results predicted by linear concentration dependence (LCD). A significant deviation of the bulk modulus from the linear concentration dependence is observed with an upward bowing parameter equal to -4.706 GPa for $SrS_{1-x}Se_x$ alloy Our results show that the bulk modulus decreases with increasing the Se concentration $x (0 \le x \le 1)$. This suggests that as x increases from x=0 (SrS), to x=1 (SrSe), $SrS_{1-x}Se_x$ becomes almost more compressible.

3.2. Electronic properties

The investigation of band gaps of SrS, SrSe and SrTe binary compounds is given for both with and without the spin-orbit coupling. Their calculated band structure energies indicate an indirect band gap $(\Gamma \rightarrow X)$.The results are given in table 2. It can be seen that the calculated energy gap values decrease with the increase of the size of the chalcogen atom. The inclusion of the spin-orbit coupling reduces the band gap by about 0.036 eV for SrS, 0.129 eV for SrSe and 0.265 eV for SrTe. By using Engel and Vosko's GGA, we have performed band structure calculations and obtained better values for band gaps, with respect to the experimental results. The results are presented in Table3.

It has been seen that the band gap values given by EVGGA are in good agreement with the experiments. In fact, it is well known that the GGA usually underestimates the experimental energy band gap [24, 25]. The GGA has a simple form which is not sufficiently flexible for accurately reproducing both exchange–correlation energy and its charge derivative. Engel and Vosko [13] by considering this short coming constructed a new functional form of the GGA which was able to better reproduce the exchange potential at the expense of less agreement in exchange energy. This approach, called EVGGA yields a better band splitting and some other properties which depend mainly on the accuracy of exchange-correlation potential. This is consistent with the results reported by Elhajhassan et al. [18, 26]. However; in this method the quantities that depend on an accurate description of exchange-energy E_x such as equilibrium volumes and bulk modulus are in minor agreement with experiment.

Table 2 **:** The calculated and experimental band gaps E_g (eV) for strontium chalcogenides at equilibrium volume.

	Present work				other work				expt.
	GGA		EVGGA		GGA		EVGGA		
	without so	with so	without so	with so	without so	with so	without so	with so	
SrS	2.536	2.500	3.389	3.355	2.25[a], 2.45[b]	2.16[a]	3.31[a]	3.20[a]	4.32[c]
SrSe	2.266	2.137	3.065	2.941	2.12[a], 2.19[b]	2.01[a]	2.95[a]	2.81[a]	3.81[c]
SrTe	1.807	1.542	2.554	2.300	1.71[a], 1.73[b]	1.38[a]	2.38[a]	2.05[a]	

[a]ref [27], [b]ref [21], [c] Ref[28]

Figure 3 shows the composition dependence of the calculated band gaps using GGA and EVGGA schemes. We calculated the total bowing parameter by fitting the non-linear variation of calculated band gaps versus concentration with quadratic function. The results go thus :

$$SrS_{1-x}Se_x \Rightarrow \begin{cases} E_g^{GGA}(x) = 2.535 - 0.311x + 0.043x^2, \\ E_g^{EVGGA}(x) = 3.395 - 0.376x + 0.038x^2, \end{cases} \qquad (1)$$

Table 3: Gap energy E_g of strontium compounds and their alloy at equilibrium volume.

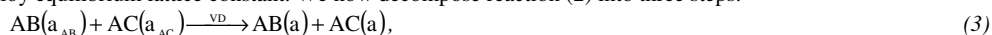| x		Eg (eV)				
		This work		other work		expt.
		GGA	EVGGA	GGA	EVGGA	
$SrS_{1-x}Se_x$	1	2.266	3.065	2.12[a], 2.19[b]	2.95[a]	3.81[c]
	0.75	2.332	3.121			
	0.5	2.386	3.218			
	0.25	2.462	3.317			
	0	2.536	3.389	2.25[a], 2.45[b]	3.31[a]	4.32[c]

[a] ref [27], [b] ref [21], [c] Ref[28]

The results of the calculated gap bowing are given in table 4. It is clearly seen that the calculated band gap exhibits weak composition dependency for $SrS_{1-x}Se_x$ alloy.

It has been seen that the main influence of the band gap energy is due to the lattice constant and the electronegativity mismatch of the parent atoms **[29, 30, 31]**. In order to better understand the physical origins of the gap bowing in this alloy, we followed the procedure of Bernard and Zunger **[32],** in which the bowing parameter *(b)* was decomposed into three physically distinct contributions**.** The overall gap bowing coefficient at x = 0.5 measures the change in band gap according to the reaction:

$$AB(a_{AB}) + AC(a_{AC}) \rightarrow AB_{0.5}C_{0.5}(a_{eq}) \qquad (2)$$

where a_{AB} and a_{AC} are the equilibrium lattice constants of the binary compounds AB and AC, respectively and a_{eq} is the alloy equilibrium lattice constant. We now decompose reaction (2) into three steps:

$$AB(a_{AB}) + AC(a_{AC}) \xrightarrow{VD} AB(a) + AC(a), \qquad (3)$$

$$AB(a) + AC(a) \xrightarrow{CE} AB_{0.5}C_{0.5}(a), \qquad (4)$$

$$AB_{0.5}C_{0.5}(a) \xrightarrow{SR} AB_{0.5}C_{0.5}(a_{eq}). \qquad (5)$$

The first step measures the volume deformation (VD) effect on the bowing. The corresponding contribution b_{VD} to the total gap bowing parameter represents the relative response of the band structure of the binary compounds AB and AC to hydrostatic pressure, which here arises from the change of their individual equilibrium lattice constants to the alloy value a = a(x) (from Vegard's rule). The second contribution, the charge-exchange (CE) contribution b_{CE}, reflects a charge transfer effect which is due to the different (averaged) bonding behavior at the lattice constant a. The final step measures changes due to the structural relaxation (SR) in passing from the unrelaxed to the relaxed alloy by b_{SR}. Consequently, the total gap bowing parameter is defined as:

$$b = b_{VD} + b_{CE} + b_{SR} \qquad (6)$$

$$b_{VD} = 2[\varepsilon_{AB}(a_{AB}) - \varepsilon_{AB}(a) + \varepsilon_{AC}(a_{AC}) - \varepsilon_{AC}(a)] \ (7)$$

$$b_{CE} = 2[\varepsilon_{AB}(a) + \varepsilon_{AC}(a) - 2\varepsilon_{ABC}(a)] \qquad (8)$$

$$b_{SR} = 4[\varepsilon_{ABC}(a) - \varepsilon_{ABC}(a_{eq})] \qquad (9)$$

where ε is the energy gap which has been calculated for the indicated atomic structures and lattice constants. Energy gaps terms in Eqs (7)-(9) are calculated separately with self-consistent band structure approach FP-LAPW. The total bowing and its three parts decomposition are listed in Table 4. It can be seen that the calculated quadratic parameters (gap bowing) within GGA and EVGGA are very close to their corresponding results obtained by Zunger approach, the agreement is also good with the relation of Tinoco et al. [33], where the bowing C is linked to the electronegativity difference Δx between the anions of constituents as follows:

$$C = \frac{5}{4}\Delta_x$$

Table 4: Decomposition of the optical bowing into volume deformation (VD), charge exchange (CE), and structural relaxation (SR) contributions
(all values are in eV).

Parameter		Calculation (Zunger approach)		Quadratic fits		b (from $C = \frac{5}{4}\Delta_\chi$)
		GGA	EVGGA	GGA	EVGGA	
SrS$_{1-x}$Se$_x$	b$_{VD}$	0.352	0.078			
	b$_{CE}$	-0.256	-0.014			
	b$_{SR}$	-0.036	-0.028			
	b	0.060	0.036	0.043	0.038	0.037

We conclude that the main contribution to the gap bowing is raised from the volume deformation b$_{VD}$. This can be clearly attributed to the large mismatch of the lattice constants of corresponding binary compounds SrS and SrSe. The charge transfer is negligible. It is due to the small electronegativity difference between S(2.58) and Se(2.55) atoms. The contribution of structural relaxation is small.
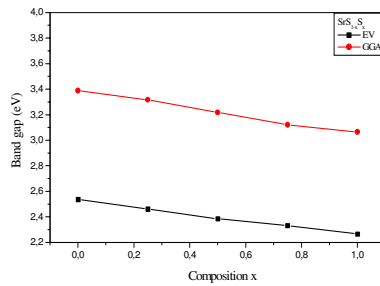

Fig. 3: Composition dependence of the calculated band gap using GGA (solid squares) and EVGGA (solid circles) for (a) SrS$_{1-x}$Se$_x$ alloy

3.3. Thermodynamic properties

In order to study the phase stability of SrS$_{1-x}$Se$_x$ alloy, we calculated the phase diagram based on the regular-solution model [34–36]. The Gibbs free energy of mixing, Δ_{Gm}, is expressed as

$$\Delta G_m = \Delta H_m - T\Delta S_m \qquad (10)$$

where

$$\Delta H_m = \Omega\, x(1-x) \qquad (11)$$

$$\Delta S_m = -R[x \ln x + (1-x)\ln(1-x)] \qquad (12)$$

ΔG_m and ΔS_m are the enthalpy and entropy of mixing, respectively; Ω is the interaction parameter which depends on the material, R the gas constant and T the absolute temperature. The mixing enthalpy of alloys can be obtained from the calculated total energies as

$$\Delta H_m = E_{AB_xC_{1-x}} - xE_{AB} - (1-x)E_{AC}, \qquad (13)$$

where $E_{AB_xC_{1-x}}$, E_{AB} and E_{AC} are the respective energies of AB_xC_{1-x} alloy and the binary compounds AB and AC. We then calculated ΔH_m to obtain Ω as a function of concentration. The interaction parameter increases almost linearly with increasing x. From a linear fit we obtained:

$$SrS_{1-x}Se_x \Rightarrow \Omega(kcal/mol) = -1.733x + 1.455$$

$$(14)$$

The average value of the x-dependent Ω in the range 0≤x≤1 obtained from these equations for $SrS_{1-x}Se$ alloy is 0.588 kcal/mol. By calculating the free energy of mixing ΔG_m at different concentrations using Eqs. (10)-(12), we determine the T–x phase diagram depicting stable, metastable and unstable mixing regions of the alloy (Fig. 6).

At a temperature lower than the critical temperature T_c, the two binodal points are determined as those points at which the common tangent line touches the ΔGm curves. The two spinodal points are determined as those points at which the second derivative of ΔGm is zero; $\partial^2(\Delta G_m)/\partial x^2 = 0$.

Figure 4 shows the calculated phase diagram including the spinodal and the binodal curves of the alloy of interest. We observed a critical temperature T_c of 148.29 K for $SrS_{1-x}Se_x$ alloy. Phase diagram shows symmetry which is due to the use of Ω as x-independent. This result is similar to the qualitative behaviour of other alloys [37-39]. The spinodal curve in the phase diagram marks the equilibrium solubility limit, i.e., the miscibility gap. For temperatures and compositions above this curve a homogeneous alloy is predicted. The wide range between spinodal and binodal curves indicates that the alloy may exist as metastable phase. Finally, our results indicate that the $SrS_{1-x}Se_x$ alloy is stable at low temperature.

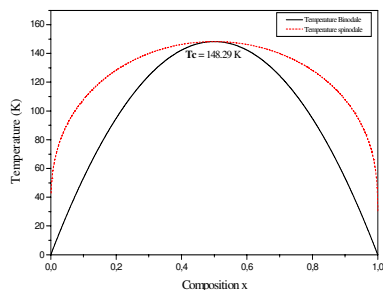Fig. 4: T–x phase diagram of $SrS_{1-x}Se_x$ ternary alloy. Solid line: binodal curve; dashedline: spinodal curve

4. Conclusion

We have made a detailed investigation of the structural and electronic properties of SrS, SrSe and SrTe binary compounds and their ternary alloy $SrS_{1-x}Se_x$ using the FP-LAPW method. The results are summarized as follows:

The lattice constant of $SrS_{1-x}Se_x$ alloy exhibits a small deviation from Vegard's law with upward bowing parameter equal to -0.043 Å. This slight deviation is mainly due to the mismatches of the lattice constants of binary compounds.

A significant deviation of the bulk modulus from LCD was found for $SrS_{1-x}Se_x$ alloy.

The spin-orbit coupling reduces the band gap, this reduction is bigger for SrTe than the other two compounds.

The calculated bowing parameter shows a strong contribution from volume deformation. This is expected due to the large mismatch of the lattice constants of the corresponding binary compounds. The band-gap bowing parameter obtained is in good agreement with the relation of Tinoco et al. [28].

The calculated phase diagram indicate a critical temperature of 148.29 K for $SrS_{1-x}Se_x$ alloy. It means that the $SrS_{1-x}Se_x$ alloy is stable at low temperature.

References

[1] Wide Band-gap Semiconductors, Edited by C.G. Van der Walle (North Holland, Amsterdam, 1993); also published as Physica B 185 (1993) 1
[2] Y. Nakanishi, T. Ito, Y. Hatanaka, G. Shimaoka, Appl. Surf. Sci. 66 (1992) 515
[3] S. Asano, N. Yamashita, Y. Nakao, Phys. Status Solidi B 89 (1978) 663
[4] R. Pandey, S. Sivaraman, J. Phys. Chem. Solids 52 (1991) 211
[5] H. Luo, R. G. Greene, A. L. Ruoff, Phys. Rev. B49 (1994) 15341
[6] C. Jain, J.R. Willis, R. Bullogh. Adv. Phys.39 (1990) 127
[7] A. Zunger, S.-H. Wei, L. G. Ferreira, J. E. Bernard, Phys. Rev. Lett. 65 (1990) 353
[8] P. Hohenberg, W. Kohn, Phys.Rev. B136 (1964) 864
[9] W. Kohn, L.J. Sham, Phys.Rev. 140 (1965) A1133
[10] P. Blaha, K. Schwarz, G.K.H. Madsen, D. Kvasnicka, J. Luitz, WIEN2k, an Augmented Plane Wave Plus Local Orbitals Program for Calculating Crystal Properties (Vienna University of Technology, Vienna, Austria, 2001)
[11] J.P. Perdew, S. Burke, M. Ernzerhof, Phys.Rev.Lett. 77 (1996) 3865
[12] J.P. Perdew, Y. Wang, Phys. Rev. B45 (1996) 13244
[13] E. Engel, S.H. Vosko, Phys Rev B47 (1991) 13164
[14] F.D. Murnaghan, Proc. Natl.Acad. Sci. USA30 (1944) 5390
[15] A. Zaoui, F. Elhaj Hassan, J. Phys: Condens.Matter 13 (2001) 253
[16] L. Vegard, Z. Phys.5 (1921) 17
[17] J. Jobst, D. Hommel, U. Lunz, T. Gerhard, G. Landwehr, Appl. Phys.Lett.69 (1996) 97
[18] F. El Haj Hassan, Phys.Stat.Sol. (b)242 (2005) 909
[19] K. Syassen, Phys. Stat. Sol. (a)91 (1985) 11
[20] H.G. Zimmer, H. Winzen, K. Syassen, Phys. Rev. B32, (1985) 4066
[21] R. Khenata, H. Baltache, M. Rerat, M. Driz, M. Sahnoun, B. Bouhafs, B. Abbar, Physica B 339 (2003) 208
[22] J. Heyd, Juan E. Peralta, Gustavo E. Scuseria, Richard L. Martin J. Chem. Phys. 123 (2005) 1
[23] P. Cortona, Inter. J. Quant. Chem. 99 (2004) 828–832
[24] P. Dufek, P. Blaha, K. Schwarz, Phys. Rev. B50 (1994) 7279
[25] G.B. Bachelet, N.E. Christensen, Phy. Rev B31 (1995) 879
[26] F. El Haj Hassan, H. Akdarzadeh, Mater. Sci. Eng. B121 (2005) 170
[27] M. Dadsetani, A. Pourghazi, Phys.Rev. B73 (2006) 195102
[28] Y.Kaneko, T. Koda. J. Cryst. Growth 86 (1988) 72
[29] Z. Charifi, H. Baaziz, N. Bouarissa, Int. J. Mod. Phys. B18 (2004) 137
[30] B. Jobst, D. Hommel, U. Lunz, T. Gerhard, G. Landwehr, Appl. Phys. Lett. 69 (1996) 97
[31] J. Van Vechten, T.K. Bergstresser, Phys. Rev. Lett. 31 (1970) 3351
[32] J. E Bernard, A. Zunger, Phys. Rev. Lett. 34 (1986) 5992
[33] T. Tinoco, M. Quintero, C. Rincon, Phys. Rev. B44 (1985) 879
[34] R.A. Swalin, Thermodynamics of Solids, Wiley, New York, (1961)
[35] L.G. Ferreira, S.H. Wei, J.E. Bernard, A. Zunger, Phys. Rev. B40 (1999) 3197
[36] L.K. Teles, J. Furthmuller, L.M.R. Scolfaro, J.R. Leite, F. Bechstedt, Phys. Rev. B62 (2000) 2475
[37] G.B. Stringfellow, J. Cryst. Growth 27 (1974) 21
[38] M. Ferhat, F. Bechstedt, Phys. Rev. B65 (2002) 75213
[39] I.-h. Ho, G. B. Stringfellow, Appl. Phys. Lett. 69 (1996) 2701